Available online at www.sciencedirect.com
ScienceDirect
J. Mater. Sci. Technol., 2010, **26**(8), 687-692.
JMST
www.JMST.org

Structure, Infrared Radiation Properties and Mössbauer Spectroscopic Investigations of $Co_{0.6}Zn_{0.4}Ni_xFe_{2-x}O_4$ Ceramics

Ying Zhang[1)†], *Jun Lin*[2)] *and Dijiang Wen*[1)]

1) Inorganic Materials Department, College of Chemistry, Chemical Engineering and Materials Science, Soochow University, Suzhou 215123, China

2) Shanghai Institute of Applied Physics, Chinese Academy of Sciences, Shanghai 201800, China

[Manuscript received December 9, 2008, in revised form September 18, 2009]

Ferrite compound $Co_{0.6}Zn_{0.4}Ni_xFe_{2-x}O_4$ was synthesized by solid state reaction. The structure and performance of $Co_{0.6}Zn_{0.4}Ni_xFe_{2-x}O_4$ compounds were studied by Mössbauer spectroscopy, X-ray diffraction (XRD), X-ray photoelectron spectroscopy (XPS) and infrared radiant tester. Mössbauer spectroscopy and XPS analysis show the valence states and distribution of cations in $Co_{0.6}Zn_{0.4}Ni_xFe_{2-x}O_4$. Zn^{2+} has invariably shown preference for the tetrahedral sites, and Ni^{2+} has the preference for the octahedral sites. The occupancy of Fe^{3+} linearly increases on the tetrahedral sites, and sharply decreases on the octahedral sites with increasing x, owing to its gradual replacement by Ni^{2+} on the octahedral sites. It indicates that due to the occupation of octahedral sites by the majority of Ni^{2+}, Fe^{3+} decreasingly migrated from the octahedral sites to the tetrahedral sites and substituted Co^{3+} sites, which made the number of Co^{3+} in the tetrahedral sites decreasing. According to the measurement results of XRD and the infrared radiant tester analysis, the lattice parameter and infrared radiance have shown a nonlinear variation, exhibiting the infrared average radiance of 0.92 in the 8–14 μm waveband, and the results demonstrate that these Co-Zn-Ni spinel ferrites have potential for application in a wide range of infrared heating and drying materials.

KEY WORDS: Infrared radiance; Mössbauer spectroscopy; NiO; Spinel ferrites

1. Introduction

At present, more and more attention has been paid to resource availability and the environment. As a result of the increasing demand for energy, more and more thermal power plants are being built. Developing advanced environmental-friendly building materials by combing functional materials has become a recent tendency. On account of the possibilities for energy conservation and reduction of pollution, infrared heating and drying technology are being used more and more in industry[1,2]. As a consequence, there is an increasing demand for high infrared radiance materials.

Infrared radiation is invisible portion of the electromagnetic spectrum beyond the red end of the visible light region. The term "infrared" refers to a broad range of frequencies in the electromagnetic spectrum, from the top end of those frequencies used for communication to the low frequency end of the visible light spectrum. The wavelength range is from 750 nm to 1 mm. The infrared segment of the electromagnetic spectrum is divided into three ranges by wavelength, measured in microns: near infrared (0.76–1.5 μm), middle infrared (1.5–5.6 μm) and far infrared (5.6–1000 μm). As the typical infrared spectrum used in military is roughly from 8 to 14 μm, we focus on infrared radiation properties of the Co-Zn spinel ferrites within 8 to 14 μm wavebands.

The family of spinel ferrite is denoted by the general formula AB_2O_4[3,4], where tetrahedral (A) sites and octahedral (B) sites are mainly divalent and trivalent cations, respectively[5,6]. A large group of 3d-

† Corresponding author. Ph. D.; Tel: +86 512 65880089; E-mail address: yingzhang@suda.edu.cn (Y. Zhang).

transition metal oxides crystallize in the spinel structure based upon the cubic close packing of oxygen ions, where the cations occupy the tetrahedral and octahedral interstices. Depending on the relative size and the minimization of the total crystalline energy, cations preferentially occupy these two locations. In actual situation, a completely random distribution occurs in most of the cases and the distribution may be represented as $(A_{1-x}B_x)_{tet}$ $[A_xB_{2-x}]_{oct}O_4$[7,8], where x is called the fraction of the tetrahedral site occupied by B cations.

The main phase of Co_2O_3-ZnO-Fe_2O_3 system ceramics is spinel type, so we consider that the infrared radiation property will be related to the crystal structure of that material, and knowledge of the structure of that is very important for controlling and forecasting infrared radiation properties of material. Under the circumstances, the crystallography, including cation distribution, of spinels has been systematized intensively. In general, different structure of spinels can be explained in terms of cation size, cation distribution in the tetrahedral site and the octahedral site, respectively.

Co_2O_3-ZnO-Fe_2O_3 system ceramics with the main phase of spinel have many beneficial properties, such as elevated thermal and chemical stabilities, good magnetism and infrared radiation properties[9,10], all of which are promising for the use of this material for infrared heating and drying applications. The dioxides of Ni are effective crystallization catalysts for the formation of spinel phase. The aim of the present work is to study the influence of Ni^{2+} on the structural and infrared radiation properties of $Co_{0.6}Zn_{0.4}Ni_xFe_{2-x}O_4$ ferrite system. Here, we report our results on the structure, cation distribution and infrared radiation properties of $Co_{0.6}Zn_{0.4}Ni_xFe_{2-x}O_4$ ferrite system by means of X-ray diffraction (XRD), Mössbauer spectroscopy, X-ray photoelectron spectroscopy (XPS) and infrared radiant tester at room temperature.

2. Experimental

2.1 Sample preparation

All samples used in this study were synthetic. $Co_{0.6}Zn_{0.4}Ni_xFe_{2-x}O_4$ (x=0.7, 0.8, 0.9) ferrites were synthesized in a polycrystalline by high temperature solid-state reaction method, which was marked as Ni0.7, Ni0.8 and Ni0.9. The oxides, Co_2O_3, ZnO, NiO and Fe_2O_3 are 99.0% pure, whereas locally available. In order to make out the difference of infrared radiation properties, we prepared the sample with x=0.0 marked as Ni0.0. The starting materials mixture in stoichiometric ratio was mixed and ground in an agate mortar, then palletized and calcined at 1573 K in air for 9 h to synthesize $Co_{0.6}Zn_{0.4}Ni_xFe_{2-x}O_4$ compounds.

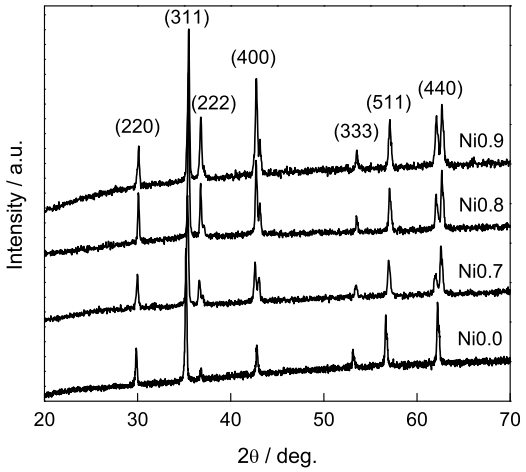

Fig. 1 X-ray diffraction patterns of the $Co_{0.6}Zn_{0.4}Ni_xFe_{2-x}O_4$ compounds

2.2 Characterization techniques

The infrared radiation properties were examined by using an infrared radiation tester (Model IRE-2, China). Phase identification and phase purity evaluation were carried out by X-ray diffraction (XRD, D/MAX-III, Japan). The valence states of elements were analyzed by X-ray photoelectron spectroscopy (XPS, VG Scientific ESCALAB 220i-XL, USA).

Mössbauer spectra were recorded in transmission mode at room temperature on a classical constant-acceleration electromechanical spectrometer using 57Co/Pb source. The velocity scale and the origin of the isomer shift were calibrated using the spectrum of a high-purity α-Fe foil. The experimental spectra were approximated by Lorentzian profile function using a standard least squares procedure. The refined hyperfine interaction parameters were: isomeric shift (δ), quadrupole splitting (ΔE), resonance line breadth ($\Gamma_{1,6}$) and relative fraction of the spectral components (A_0).

3. Results and Discussion

3.1 XRD patterns analysis

The recorded XRD patterns are shown in Fig. 1. The main reflections from crystal planes (220), (311), (222), (400), (511) and (440) characterizing spinel ferrites are observed in Fig. 1. The reflections from the other crystal planes, such as (333), also can be observed but with weak intensities. The analysis of XRD patterns indicated that the ferrite samples have spinel cubic structure.

3.2 Infrared radiation property analysis

Table 1 shows the infrared average radiance in

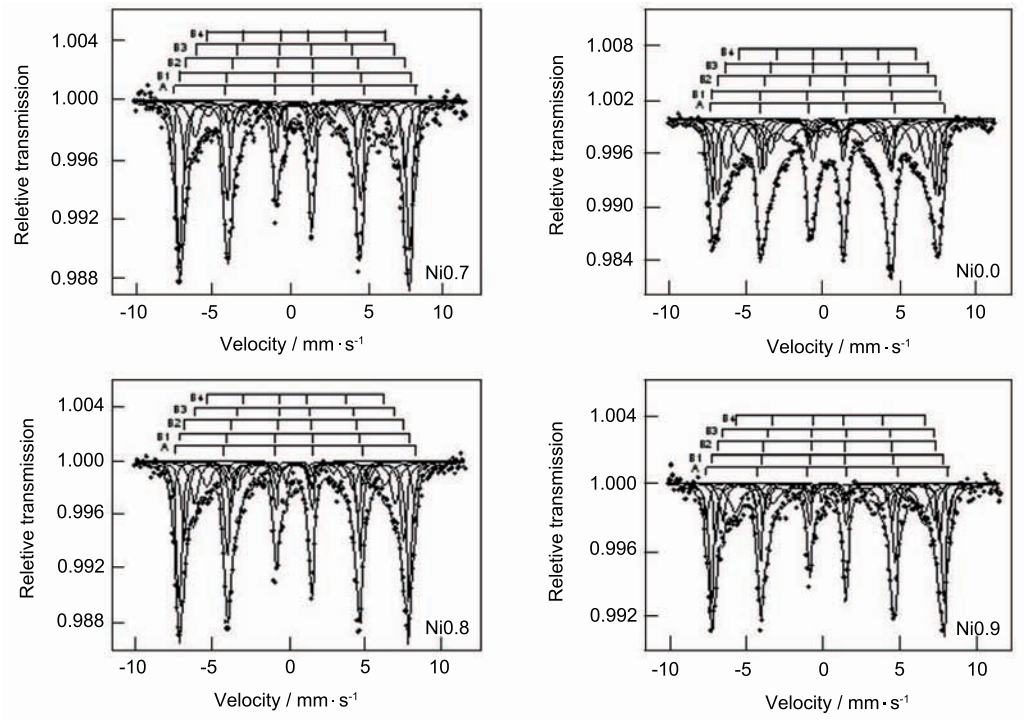

Fig. 2 The room temperature Mössbauer spectra of the $Co_{0.6}Zn_{0.4}Ni_xFe_{2-x}O_4$ (x=0.0, 0.7, 0.8, 0.9) ferrites with x. The black dots represent the experimental datum points; The solid lines through the data points are the results of the least-squares fitting to the experimental data

Table 1 Infrared radiance (ε) and lattice constants (a) of $Co_{0.6}Zn_{0.4}Ni_xFe_{2-x}O_4$ compounds

Samples	ε	a/nm
Ni0.0	0.891(3)	0.8432(5)
Ni0.7	0.902(1)	0.8396(1)
Ni0.8	0.920(2)	0.8384(2)
Ni0.9	0.907(1)	0.8385(7)

the 8–14 μm waveband and lattice parameter of the $Co_{0.6}Zn_{0.4}Ni_xFe_{2-x}O_4$ samples. As can be obtained from Table 1, the infrared radiance of the Ni0.0 is lower. With increasing the doped Ni ions, the infrared radiance increases obviously. But the increase of radiance is limited by the content of Ni^{2+} ions, and the better radiance appears in sample Ni0.8.

The lattice parameter of the cubic crystal of the $Co_{0.6}Zn_{0.4}Ni_xFe_{2-x}O_4$ spinel solid solution obeys the Bragg′s law. The lattice parameter a was calculated from each crystal plane. The average lattice parameter a may be obtained by calculating the average of a values of each sample. The relation between infrared radiance and lattice parameter is shown in Table 1, which represents nonlinear variation of infrared radiance with lattice parameter. The lattice parameter a decreases with increasing Ni^{2+} ions doped compared to precursor Ni0.0, up to 0.8384 nm when x is 0.8 and the infrared radiance changes reversely at the same time. It is clear that the infrared radiance increases as the Ni^{2+} content increases and the lattice parameter decreases in this experiment. The maximum value of infrared radiance is 0.92 when x is 0.8. From the initial (Ni0.0) to the final composition (Ni0.9) of the samples, the lattice parameter has decrease from 0.8432 to 0.8384 nm, while the infrared radiance slightly increases from 0.891 to 0.920 due to the different cation distribution on the A-site and B-site.

3.3 Mössbauer spectra analysis

Mössbauer spectra of Ni0.0, Ni0.7, Ni0.8 and Ni0.9 samples were recorded at room temperature by using a computerized Mössbauer spectrometer of the electromechanical type in constant acceleration mode.

Figure 2 shows the recorded Mössbauer spectra for all samples. The Mössbauer spectra were analyzed by a least-squares fitting computer program. The analysis of the spectral lines for the all samples shows a good match to six-line Zeeman patterns. The sample corresponding to Ni0.0 shows rather broad lines. The spectra for Ni0.7, Ni0.8 and Ni0.9 show very similar spectra. Each one shows two quadrupole doublets: one due to the tetrahedral site (A-site) and the other due to the octahedral site (B-site).

The samples show that the lines of the B-site patterns are broadened and certain overlapping appears, so the B-site pattern is fitted into several components to obtain the B-site subpatterns[11]. The appearance of several components is due to the different cations at the A-site. In our study, the A-site is occupied by Fe^{3+}, Zn^{2+} and Co^{3+} ions, and the B-site cation must be different number of Fe^{3+}, Ni^{2+} and Co^{3+} ions.

Table 2 Mössbauer parameters of the system $Co_{0.6}Zn_{0.4}Ni_xFe_{2-x}O_4$, where B_n (n=0, 1, 2, 3, and 4) represents the B-site Fe ions with Ni nearest neighbors. The parameters δ, ΔE, H, A_0 and $\Gamma_{1,6}$ represent the isomer shift, quadrupole shift, hyperfine field, fractional area and the outermost line of the samples, respectively

Samples	Subpatterns	δ/(mm/s)	ΔE/(mm/s)	H/T	A_0/%	$\Gamma_{1,6}$/(mm/s)
Ni0.0	A	0.30	−0.04	47.5	5	0.30
	B0	0.24	0.01	46.0	16	0.39
	B1	0.30	−0.05	44.1	20	0.50
	B2	0.35	−0.06	40.7	19	0.74
	B3	0.32	−0.01	35.7	15	0.89
	B4	0.33	0.06	27.2	17	1.21
Ni0.7	A	0.28	0.01	49.0	7	0.32
	B0	0.28	0.04	46.6	41	0.47
	B1	0.33	0.03	44.5	19	0.45
	B2	0.34	−0.02	40.2	15	0.72
	B3	0.33	0.15	35.7	8	0.98
	B4	0.46	0.70	29.3	8	0.63
Ni0.8	A	0.27	0.03	49.1	8	0.39
	B0	0.28	0.02	46.8	34	0.41
	B1	0.30	−0.01	44.7	22	0.46
	B2	0.35	−0.03	40.9	15	0.60
	B3	0.32	0.18	36.2	12	0.81
	B4	0.44	0.45	28.5	7	0.59
Ni0.9	A	0.28	0.01	49.1	10	0.40
	B0	0.29	0.01	46.9	34	0.38
	B1	0.28	0.02	45.2	14	0.31
	B2	0.35	−0.02	42.8	13	0.46
	B3	0.36	0.13	38.2	20	0.96
	B4	0.46	0.50	27.8	7	0.67
Error		±0.02	±0.02	±0.2	±0.02	±0.02

Table 3 Cation distributions of $Co_{0.6}Zn_{0.4}Ni_xFe_{2-x}O_4$ compounds

Samples	Cation distribution	
	Tetrahedral A-site	Octahedral B-site
Ni0.0	$Co^{3+}0.5Zn^{2+}_{0.4}Fe^{3+}_{0.1}$	$Co^{3+}_{0.1}Fe^{3+}_{1.9}$
Ni0.7	$Co^{3+}_{0.46}Zn^{2+}_{0.4}Fe^{3+}_{0.14}$	$Co^{3+}_{0.14}Ni^{2+}_{0.7}Fe^{3+}_{1.16}$
Ni0.8	$Co_{0.44}Zn_{0.4}Fe_{0.16}$	$Co^{3+}_{0.16}Ni^{2+}_{0.8}Fe^{3+}_{1.04}$
Ni0.9	$Co^{3+}_{0.4}Zn^{2+}_{0.4}Fe^{3+}_{0.2}$	$Co^{3+}_{0.2}Ni^{2+}_{0.9}Fe^{3+}_{0.9}$

The Mössbauer parameters determined from the above mentioned subpatterns are listed in Table 2.

Table 2 illustrates that the A-site has the largest hyperfine field H_A and its isomer shift δ_A indicates pure Fe^{3+} ions. The isomer shift δ_B of the B-site patterns may indicate a mixed valence state of Fe^{3+} and Fe^{2+} ions. This state is associated with fast electron hopping between the neighboring Fe^{3+} and Fe^{2+} ions at B-site. The isomer shift δ_A is less than δ_B, maybe due to the difference in Fe^{3+}-O^{2-} internuclear separations. This bond separation is small for A-site, because there is a larger overlapping of electronic orbit of Fe^{3+} and O^{2-} at the A-site[12]. This results in a larger covalence and hence smaller δ_A. The data of the quadrupole shift ΔE shows a mulriple change from the cubic spinel structure. Generally, the A-site ΔE derives from the asymmetrical charge distribution surrounding the iron ion. The B-site has trigonal point symmetry and exhibits an electric field gradient along (111) direction. Table 2 indicates that the outermost line width $\Gamma_{1,6}$ of the A-site pattern is less than that of the B-site subpatterns, which is attributed to cation distribution of Fe^{3+}, Zn^{2+} and Co^{3+} ions at the A-site. The hyperfine field at the A-site is larger than that at the B-site. Both H_A and H_B increase with increasing x, which can be explained by super exchange interaction and cation distribution[13].

So the cation distribution can be deduced from the area under the patterns belonging to A and B sublattice and from the preference of the element site[14]. It is known that the Zn^{2+} ions have powerful preference for the A-site and the Ni^{2+} ions for the B-site[15]. While the Fe^{3+} and Co^{3+} ions substitute on both A and B sites.

From the obtained result, cation distribution about octahedral and tetrahedral sites can be denoted as $(Co_{0.6-y}Zn_{0.4}Fe_y)_{tet}[Co_yNi_xFe_{2-x-y}]_{oct}$, where x is the content of Ni^{2+} doped and y is the fractional area of the samples. Several cation distributions deduced are listed in Table 3, which makes it clear that

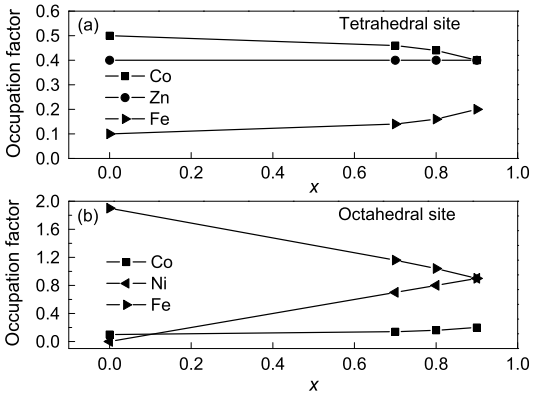

Fig. 3 Variation of cation occupation tetrahedral site (a) and octahedral site (b) factor with content of Ni^{2+} doped

Ni^{2+} ions exist in the B-site, and substitute the Fe^{3+}. It is obvious from Table 3 that the cations have shown a complex preference order about site. With increasing x, each of the cation has shown different degree of preference for both the A-site and B-site excepting Zn^{2+}, which has invariably shown a preference for the A-site and the Ni^{2+} has the preference for the B-site. The variation of the occupation factor of individual cation in the tetrahedral and octahedral sites is shown in Fig. 3.

It is evident from Fig. 3 that different cations have shown different nature of variation with increasing substitution, which indicated by the regression curve fitting the experimental data. The occupancy of Fe^{3+} ions near-linearly increases on the A-site, and sharply decreases on the B-site with increasing x owing to its gradual replacement by Ni^{2+} ions on the B-site. It indicates that due to the occupation of octahedral site by a great many Ni^{2+} ions, Fe^{3+} ions decreasingly migrate from the octahedral site to the tetrahedral site and substitute the Co^{3+} ions, which makes the number of Co^{3+} ions in the tetrahedral site decreasing. The substitution of divalent Ni^{2+} ions in Co-Zn ferrite system decreases the lattice parameter of the system, and increases the infrared radiation properties, maybe due to the structure cell volume contraction and original lattice vibration periodically being destroyed[16].

3.4 XPS analysis

In order to verify the correctness of the results by Mössbauer spectra, we investigated the electrode surface by XPS analysis. Figure 4 shows four survey spectra for $Co_{0.6}Zn_{0.4}Ni_xFe_{2-x}O_4$ ferrites with x=0.8.

We have observed that the binding energy for the $Fe2p_{3/2}$ was 710.6 eV, corresponding to $2p_{3/2}$ of Fe_2O_3, so we would believed that Fe has the Fe^{3+} oxidation state existence. In the same way, the binding energy for the $Co2p_{3/2}$ was 779.2 eV, corresponding to $2p_{3/2}$ of Co_2O_3, so we would believe that Co has the Co^{3+} oxidation state existence. The binding energy for the $Zn2p_{3/2}$ was 1020.8 eV, corresponding to $2p_{3/2}$ of ZnO, so we can deduce that Zn has the Zn^{2+} oxidation state existence. The binding energy for the $Ni2p_{3/2}$ was 853.9 eV, corresponding to $2p_{3/2}$ of NiO,

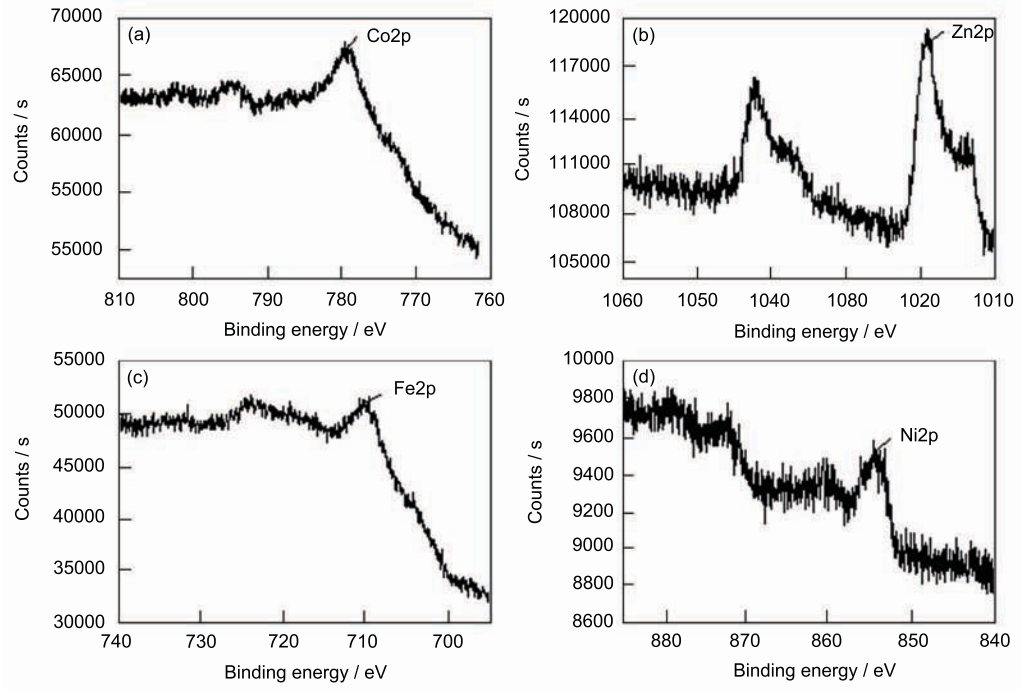

Fig. 4 Co2p(a), Zn2p (b), Fe2p (c) and Ni2p (d) XPS survey spectra of the $Co_{0.6}Zn_{0.4}Ni_xFe_{2-x}O_4$ ferrites with x=0.8

so we would believe that Ni has the Ni^{2+} oxidation state existence[17,18]. This result of valence states of elements is in good agreement with Mössbauer spectra analysis.

4. Conclusions

(1) XRD shows only a single spinel cubic phase is present for all studied compositions.

(2) The valence of elements in $Co_{0.6}Zn_{0.4}Ni_xFe_{2-x}O_4$ system was determined by XPS and Mössbauer analysis.

(3) Mössbauer analysis shows that the four cations in the $Co_{0.6}Zn_{0.4}Ni_xFe_{2-x}O_4$ system have shown different site preferences with increasing Ni^{2+} ions. Zn^{2+} ions have occupied the tetrahedral site in invariable proportions, and the Co^{3+}, Fe^{3+} ions have occupied the A-site and B-site in diverse proportions.

(4) The infrared radiance is 0.920 in the 8–14 μm waveband when x=0.8. The substitution of divalent Ni^{2+} ions in Co-Zn ferrite system decreases the lattice parameter of the system, and increases the infrared radiation properties.

Acknowledgement

This research was supported by the Key Project in Science and Technology Innovation Cultivation Program of Soochow University, China (Contract No. Q3109808).

REFERENCES

[1] S.M. Wang and K.M. Liang: *J. Non-Cryst. Solids,* 2008, **354**, 1522.

[2] J.S. Liang, L.J. Wang and G.K. Xu: *J. Rare Earth.,* 2006, **24**, 281.

[3] X.H. Wei, D.H. Chen and W.J. Tang: *Mater. Chem. Phys.,* 2007, **103**, 54.

[4] V.L. Mathe and R.B. Kamble: *Mater. Res. Bull.,* 2008, **43**, 2160.

[5] Z.B. Wang, C.H. Zhao, P.H. Yang and A.J.A. Winnubst: *J. Eur. Ceram. Soc.,* 2006, **26**, 2833.

[6] H.M. Zaki and S.F. Mansour: *J. Phys. Chem. Solids,* 2006, **67**, 1643.

[7] K.H. Roumaih, R.A. Manapov and E.K. Sadykov: *J. Magn. Magn. Mater.,* 2005, **288**, 2675.

[8] G. Avdeev, K. Petrov and I. Mitov: *Solid State Sci.,* 2007, **9**, 1135.

[9] O. Suwalka, R.K. Sharma, V. Sebastian and N.K. Lakshmi: *J. Magn. Magn. Mater.,* 2007, **313**, 198.

[10] R.N. Bhowmika, R. Ranganathana, B. Ghoshb and S. Kumarb: *J. Alloy. Compd.,* 2008, **456**, 348.

[11] M.A. Amer and M.El Hiti: *J. Magn. Magn. Mater.,* 2001, **234**, 118.

[12] V.T. Thanki, K.H. Jani, B.S. Trivedi, K.B. Modi and H.H. Joshi: *Mater. Lett.,* 1998, **37**, 236.

[13] K.P. Thummer, M.C. Chhantbar, K.B. Modi and G.J. Baldha: *Mater. Lett.,* 2004, **58**, 2248.

[14] E.J. Choi, Y.K. Ahn and K.C. Song: *J. Magn. Magn. Mater.,* 2006, **301**, 171.

[15] P.W. Lu: *Fundamentals of Abio-materials Science,* Wuhan University of Technology Press, Wuhan, 1996. (in Chinese)

[16] X.F. Liu, F. Zhang and H.J. Sun: *Funct. Mater.,* 2003, **88**, 34.

[17] A.C. Tavares, M.I. da Silva Pereira, M.H. Mendonä, M.R. Nunes, F.M. Costa and C.M. Sá: *J. Electroanal. Chem.,* 1998, **449**, 91.

[18] A.C. Tavares, M.A.M. Cartaxo, M.I. da Silva Pereira and F.M. Costa: *J. Electroanal. Chem.,* 1999, **464**, 187.